

**Supporting Information**

**Unexpected discovery of low-cost maricite NaFePO<sub>4</sub> as a high-performance electrode for Na-ion batteries**

*Jongsoon Kim<sup>a†</sup>, Dong-Hwa Seo<sup>b†</sup>, Hyungsub Kim<sup>b</sup>, Inchul Park<sup>b,c</sup>, Jung-Keun Yoo<sup>d</sup>, Sung-Kyun Jung<sup>b</sup>, Young-Uk Park<sup>b,c</sup>, William A. Goddard III<sup>e</sup>, and Kisuk Kang<sup>b,c\*</sup>*

<sup>a</sup> Korea Atomic Energy Research Institute (KAERI), P.O. Box 105, Yuseong-gu, Daejeon 305-600,

<sup>b</sup> Korea Department of Materials Science and Engineering, Research Institute of Advanced Materials, Seoul National University, 599 Gwanak-ro, Gwanak-gu, Seoul 151-742, Korea

<sup>c</sup> Center for Nanoparticle Research, Institute for Basic Science, Seoul National University, Seoul, 151-742, Korea

<sup>d</sup> Department of Materials Science and Engineering, Korea Advanced Institute of Science and Technology (KAIST), 291 Daehak-ro, Yuseong-gu, Daejeon 305-701, Korea

<sup>e</sup> Materials and Process Simulation Center (MC 139-74), California Institute of Technology, 12000 East California Boulevard, Pasadena, CA, 91125, USA.

Corresponding Author: Prof. Kisuk Kang

E-mail: [matlgen1@snu.ac.kr](mailto:matlgen1@snu.ac.kr)

TEL: +82-2-880-7088

## **S1. Experimental**

### **S1. 1. The synthesis of maricite NaFePO<sub>4</sub>**

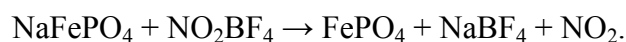
Na<sub>2</sub>CO<sub>3</sub> (Sigma Aldrich, 99%), FeC<sub>2</sub>O<sub>4</sub>·2H<sub>2</sub>O (Sigma Aldrich, 99%), and NH<sub>4</sub>H<sub>2</sub>PO<sub>4</sub> (Fluka, 98%) with molar ratios of 0.5 : 1 : 1 were used as precursors. They were thoroughly mixed and grounded by high energy ball-milling (HEBM) at 500 rpm over 24 hours. The mixed precursors were then fired at 350°C under Ar conditions for 5 hours. The mixture was then re-ground and manually pelletized using a disk-shaped mold. After pre-heating, we calcined the pellet at 600°C under Ar conditions for 10 hours.

### **S1. 2. Reducing particle size and improving electric conductivity of maricite NaFePO<sub>4</sub>**

The powder had been well blended with 20 wt% Super P through dry ball-milling at 200 rpm over 12 hours, using planetary ball-milling (pulverisette 5, Fritsch).

### **S1. 3. Fully desodiation of maricite NaFePO<sub>4</sub>**

Fully desodiated samples, FePO<sub>4</sub>, were prepared using stoichiometric amounts of NO<sub>2</sub>BF<sub>4</sub> (95 %, Aldrich) in acetonitrile solvent (anhydrous, 99.8 %, Aldrich) according to the following reaction:



NO<sub>2</sub>BF<sub>4</sub> is a strong oxidizing agent equivalent to a 4.8 V potential versus Na<sup>+</sup> / Na. The solution was maintained at 60 °C for 100 h. Final products of the desodiated phases were obtained by washing with acetonitrile using a centrifuge.

#### **S1. 4. Materials characterization**

The stoichiometry of the delithiated compound was determined by inductively coupled plasma-atomic emission spectroscopy (ICP-AES). Powder XRD was carried out on a Bruker D8-Advantage powder diffractometer using Cu K $\alpha$  radiation (= 1.54178 Å) from 2 $\theta$  =10 to 60 ° at 1s per step of 0.01°. Fe K-edge X-ray absorption spectra (XAS) were taken on the 10C beamline at the Pohang Accelerator Laboratory (PAL). Fe K-edge energy calibration was performed using Fe metal foil as reference. A reference spectrum was simultaneously recorded for *in-situ* spectrum using Fe metal foil. Thermal-gravimetric analysis (TGA) was performed under an air condition at a heating rate of 10 °C min<sup>-1</sup> using a Labsys.Evo (SETARAM, France) from room temperature to 900 °C. Carbon analysis was performed using Carbon determinator CS800 (Eltra).

#### **S1. 5. Electrochemistry**

Electrochemical tests were performed in a CR2016-type coin cell assembled in an Ar-filled glove-box. The slurry of 80 wt% C-coated NaFePO<sub>4</sub>, 10 wt% carbon black (Super-P), and 10 wt% polyvinylidene fluoride dispersed in N-methyl-2-pyrrolidone (NMP) was prepared and cast on aluminum foil. (The final content of the carbon added is 26 wt% of the electrode) NMP was evaporated at 120°C for 2 hours. The mass loading of the electrode is 2.5 mg·cm<sup>-2</sup>. Na cell was assembled in a CR2032 type coin cell with a Na counter electrode, separator (Celgard 2400), and 1M NaPF<sub>6</sub> electrolyte in a mixture of EC/PC (1:1) in an Ar-filled glove box. Li cell was assembled in a CR2032 type coin cell with a Li counter electrode, separator (Celgard 2400), and 1M LiPF<sub>6</sub> electrolyte in a mixture of EC/DMC (1:1) in an Ar-filled glove box. GITT measured at C/20 rate by the intermittent charge mode and one hour

of rest period ( $dV/dt \sim 10^{-6} \text{ V s}^{-1}$ ) is introduced during a charging step. The charge/discharge test was performed using a galvanostat (WonA Tech).

## **S2: Computational details**

### **S2.1. Density functional theory calculations**

Density functional theory (DFT) calculations were conducted using the spin-polarized generalized gradient approximation (GGA) with a Perdew-Burke-Ernzerhof (PBE) functional.<sup>1</sup> We used the Vienna *ab initio* simulation package (VASP), in which a plane-wave basis set and the projector-augmented wave (PAW) method were implemented.<sup>2</sup> Hubbard U parameters (GGA+U) were applied to correct for self-interaction errors within the GGA.<sup>3</sup> An effective U value of 4.3 eV was used for Fe ion.<sup>4</sup> A plane-wave basis set with a kinetic-energy cutoff of 520 eV and  $2 \times 3 \times 4$  or  $2 \times 2 \times 2$  Monkhorst-Pack  $k$ -point meshes were used to ensure that the total energies converged to less than 5 meV per formula unit (*fu*).

### **S2.2. Nudged elastic band (NEB) calculations**

The Na diffusivity in  $\text{Na}_{1-x}\text{FePO}_4$  was estimated from the QM calculations. We used the nudged elastic band (NEB) method to determine the activation barriers for Na/Li hopping between stable sites. The activation barriers of Na were calculated in the dilute vacancy (or dilute Na) limit with 1 vacancy (or 1 Na) in the  $1 \times 2 \times 2$  supercells containing 16 formula unit of  $\text{Na}_{1-x}\text{FePO}_4$ . All lattice parameters were fixed at fully relaxed  $\text{Na}_{15/16}\text{FePO}_4$  and  $\text{Na}_{1/16}\text{FePO}_4$  from the QM; all internal degrees of freedom were relaxed during NEB calculations. The NEB calculations, which started with five replicas of each system, initiated

by the linear interpolation between the initial and final states of the diffusion pathways, were performed within the GGA approximation instead of the GGA+U approximation to exclude the interaction between Na diffusion and the charge transfer processes. Li diffusivity in  $\text{Li}_{1-x}\text{FePO}_4$  was estimated in a similar manner.

### S2.3. Multiscale methods to investigate Na diffusion in $\alpha\text{-FePO}_4$

- 1) Constructing the amorphous structure of  $\text{FePO}_4$  by a melt-and-quenching process

*Ab initio* molecular dynamics (AIMD) calculations were used to construct  $\alpha\text{-FePO}_4$  structure via melt-and-quenching. AIMD calculations were performed using the PBE functional with the NVT (canonical) ensemble, as implemented in VASP. During AIMD, the lattice parameters were fixed in a fully relaxed state of olivine  $\text{FePO}_4$  within the GGA. The  $1 \times 2 \times 2$  supercell of olivine  $\text{FePO}_4$  was adopted as a starting point of the AIMD. At first, we held the temperature at 2500 K to mimic the liquid state of  $\text{FePO}_4$ . Three  $\alpha\text{-FePO}_4$  samples were prepared using three holding times (10, 15 and 20 ps) at 2500 K, as shown in Supporting Figure S2. The melted structure was quenched to room temperature (300 K) and then allowed to relax fully (within the GGA). The time step and quenching rate were 0.5 fs and 100 K  $\text{ps}^{-1}$  at high temperature (1000 - 2500 K) and 1 fs and 35 K  $\text{ps}^{-1}$  at low temperature (300 –1000 K). Amorphization of  $\text{FePO}_4$  was confirmed by the radial distribution function (RDF). Supporting Figure S3 shows the RDFs of olivine  $\text{FePO}_4$  and  $\alpha\text{-FePO}_4$ , indicating that olivine  $\text{FePO}_4$  was well crystallized, whereas  $\alpha\text{-FePO}_4$  was fully disordered.

- 2) Finding stable Na sites in  $\alpha\text{-FePO}_4$

Stable Na sites in  $\alpha$ -FePO<sub>4</sub> were identified by grand canonical Monte Carlo (GCMC) simulations. The GCMC simulations were performed at 600 K with the sorption module within the Cerius 2 software package [Cerius2 Software, version 4.10, Accelrys Inc.: San Diego, CA.] using the DREIDING force-field parameters for the Li-O interaction.<sup>5</sup> We carried out GCMC simulations on three samples of  $\alpha$ -FePO<sub>4</sub> constructed by AIMD and found 16 stable Na sites for each system. The Na site energies were evaluated by positioning one Na ion at one of the 16 sites identified and comparing the DFT energies of Na<sub>1/16</sub>FePO<sub>4</sub>.

### 3) Visualizing plausible Na diffusion pathways

The possible Na diffusion pathways of the electrode materials were estimated using the bond-valence summation (BVS) method.<sup>6, 7</sup> The BV sum of the Na ions in the structure was calculated by summing up the bond-valence of Na to all oxygen ions within 7.5 Å at each grid point. The Na ion was located in the areas of low BV mismatch compared with ideal valence conditions (Na: 1+) in the structure; thus, the Na ion migrated along the low BV mismatch areas. The BV mismatch maps of the three samples of  $\alpha$ -FePO<sub>4</sub> and olivine FePO<sub>4</sub> were constructed using the 3DBVSMAPPER program<sup>8</sup> and drawn by VESTA program<sup>9</sup>, as shown in Figure 4 and Figure S4.

### 4) Estimating the activation barriers of Na hopping

We excluded any Na sites, whose the site energies were 1 eV higher than the most stable Na site. Then, we chose every pair of Na sites within 5 Å, and calculated the activation energies for Na hopping using the NEB method, if the two sites were connected to each other

within the BV mismatch maps. Because there were no representative diffusion pathways, statistical evaluation with more than one  $\alpha$ -FePO<sub>4</sub> sample and a diffusion pathway was required to estimate the activation energies of Na hopping in the amorphous structure.

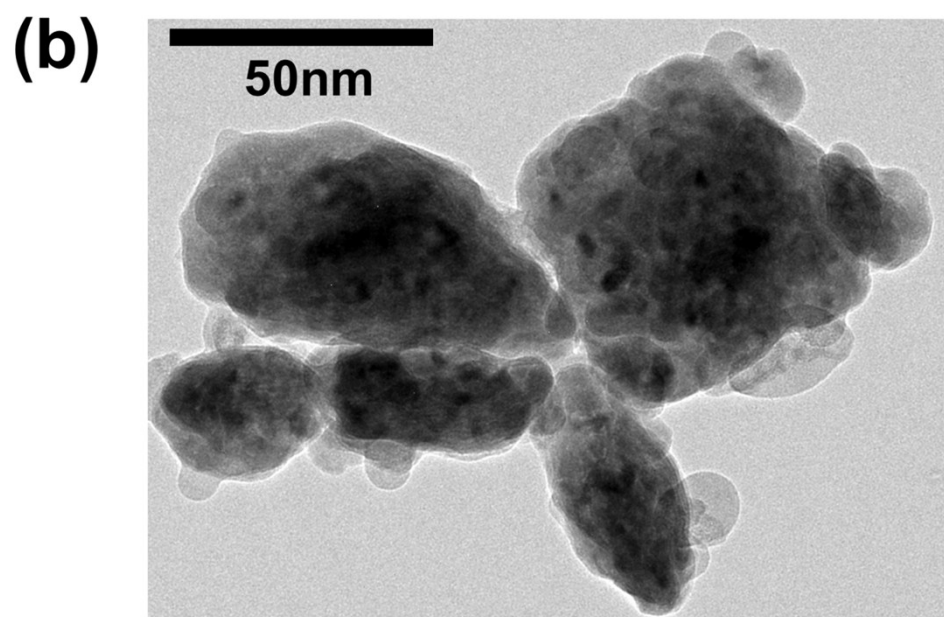
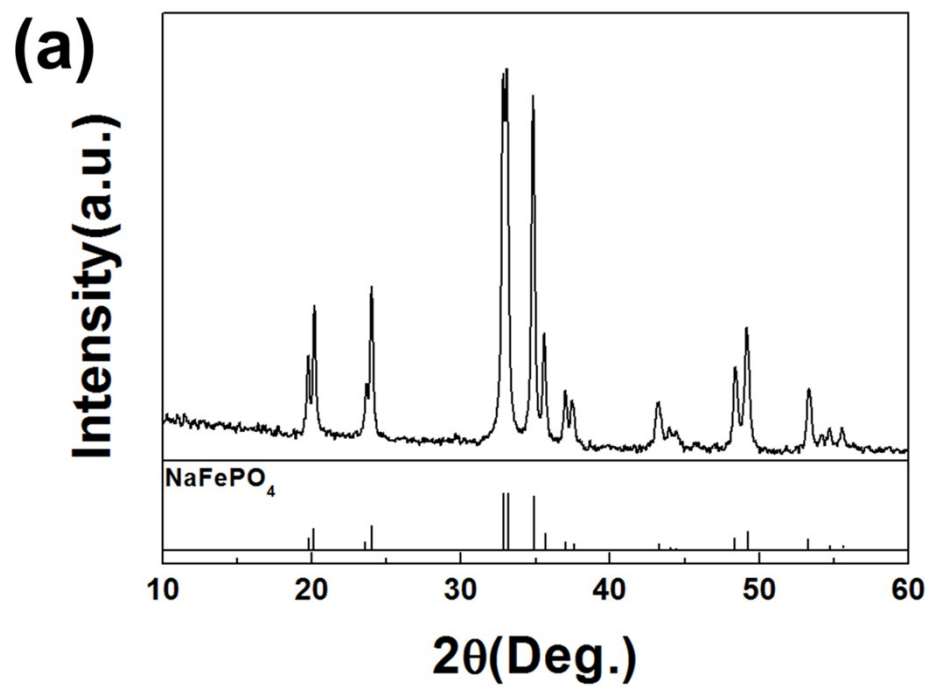


**Figure S1.** The XRD pattern and TEM image of C-NaFePO<sub>4</sub>

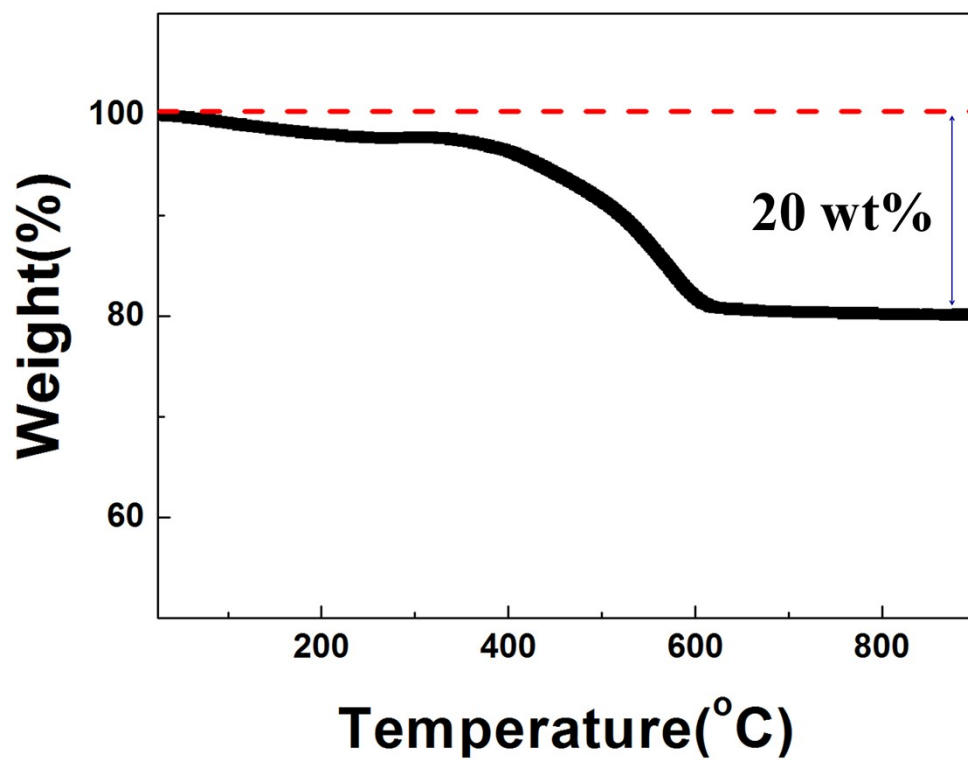


**Figure S2.** The TGA analysis of C-NaFePO<sub>4</sub>

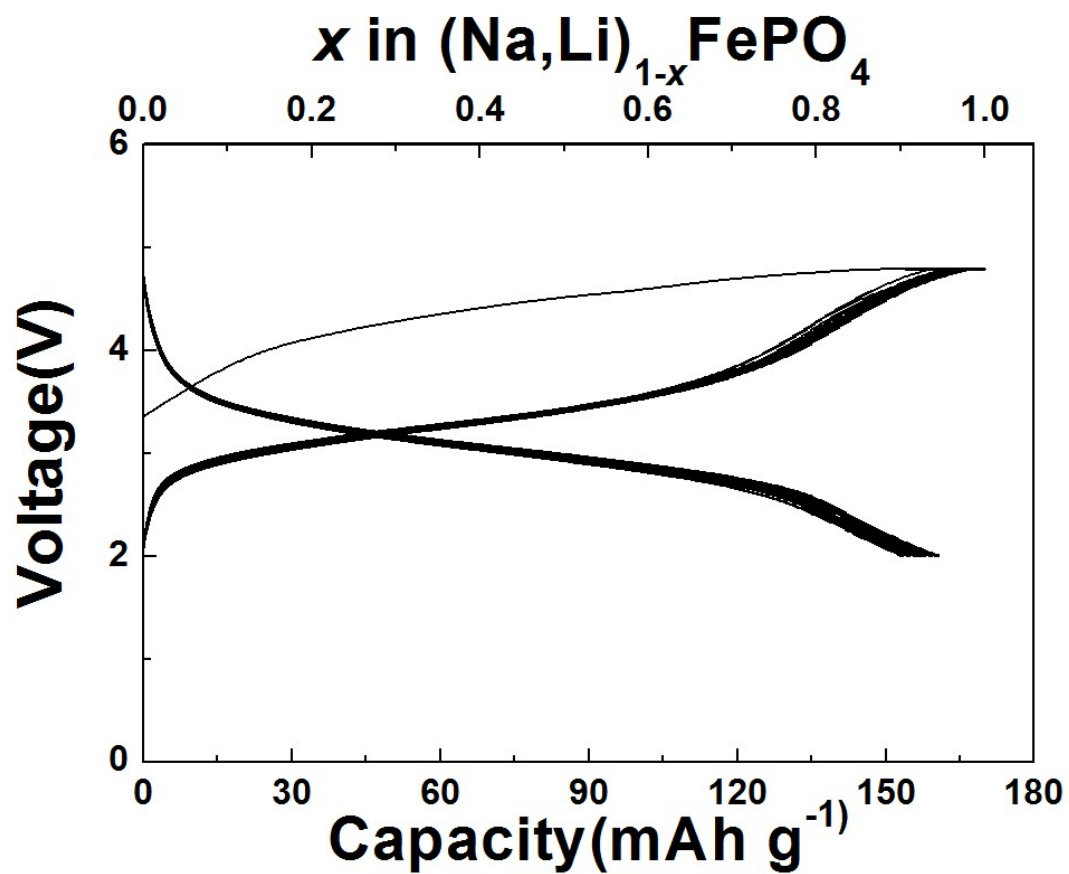


**Figure S3.** (a) Galvanostatic curves of maricite  $\text{NaFePO}_4$  over 100 cycles at C/20 in Li cell (charging under CCCV mode (C/20 rate from 4.8V to 2.0V and 5 hour holding at 4.8V))

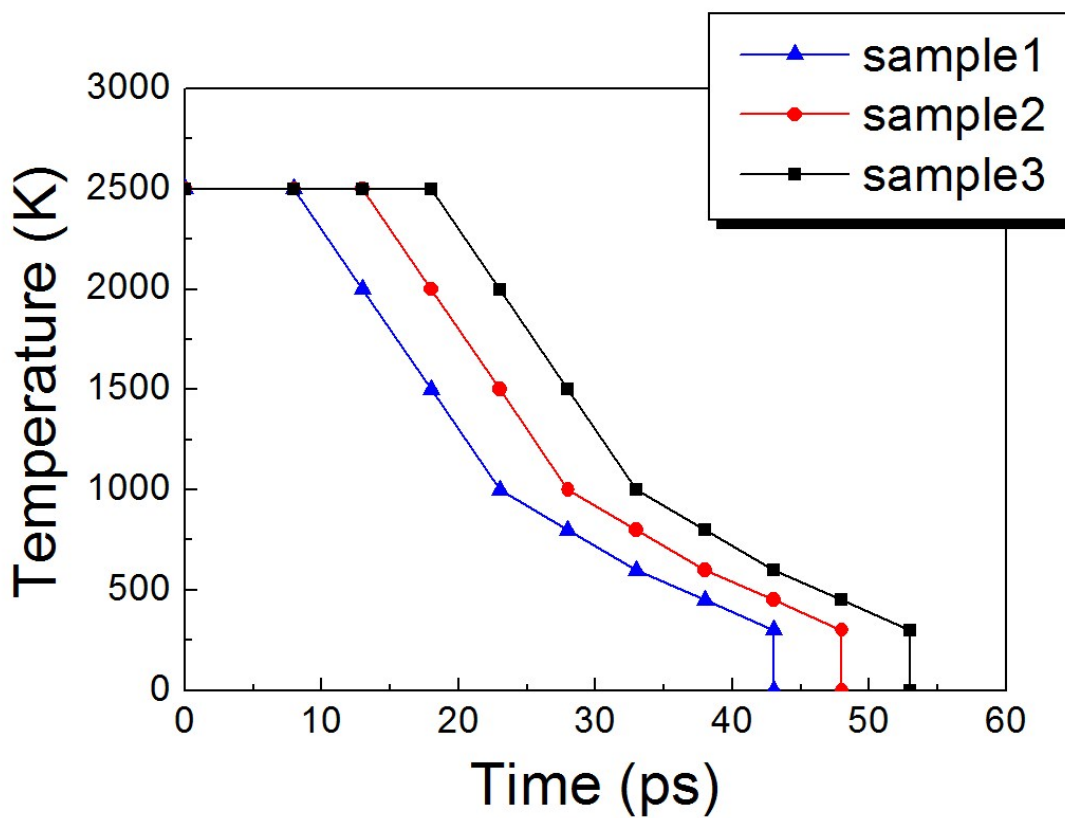


**Figure S4.** The melt-and-quenching process used to prepare amorphous  $\text{FePO}_4$  structure with three different holding times at high temperature.

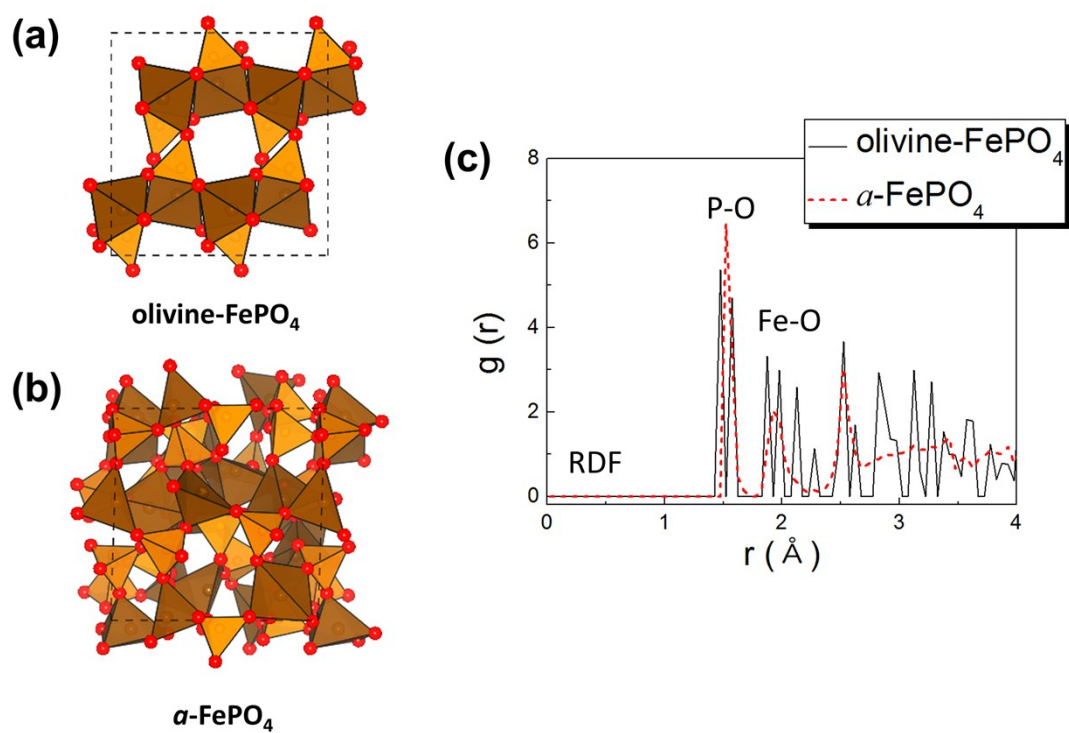


**Figure S5.** The structural difference between olivine  $\text{FePO}_4$  and  $\alpha\text{-FePO}_4$ . The structure of (a) olivine  $\text{FePO}_4$  and (b)  $\alpha\text{-FePO}_4$ . (c) Radial distribution functions (RDF) of olivine  $\text{FePO}_4$  (solid line) and  $\alpha\text{-FePO}_4$  (dashed line). Brown polyhedra indicate  $\text{FeO}_x$  and orange tetrahedra indicate  $\text{PO}_4$ .

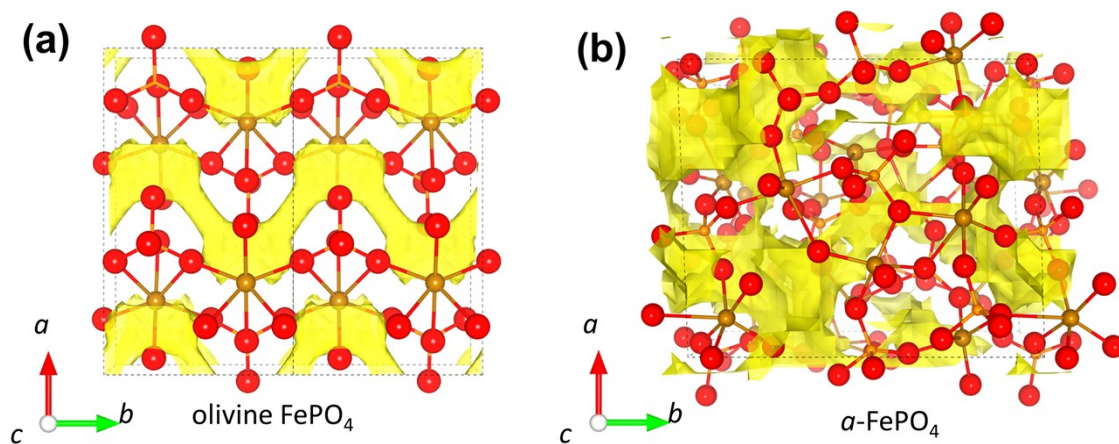


**Figure S6.** The plausible diffusion pathways of olivine FePO<sub>4</sub> and  $\alpha$ -FePO<sub>4</sub>, which were determined by bond valence summation (BVS) method. Yellow isosurfaces indicate plausible Na diffusion pathways. Brown balls and red balls indicate Fe and O atoms, respectively.

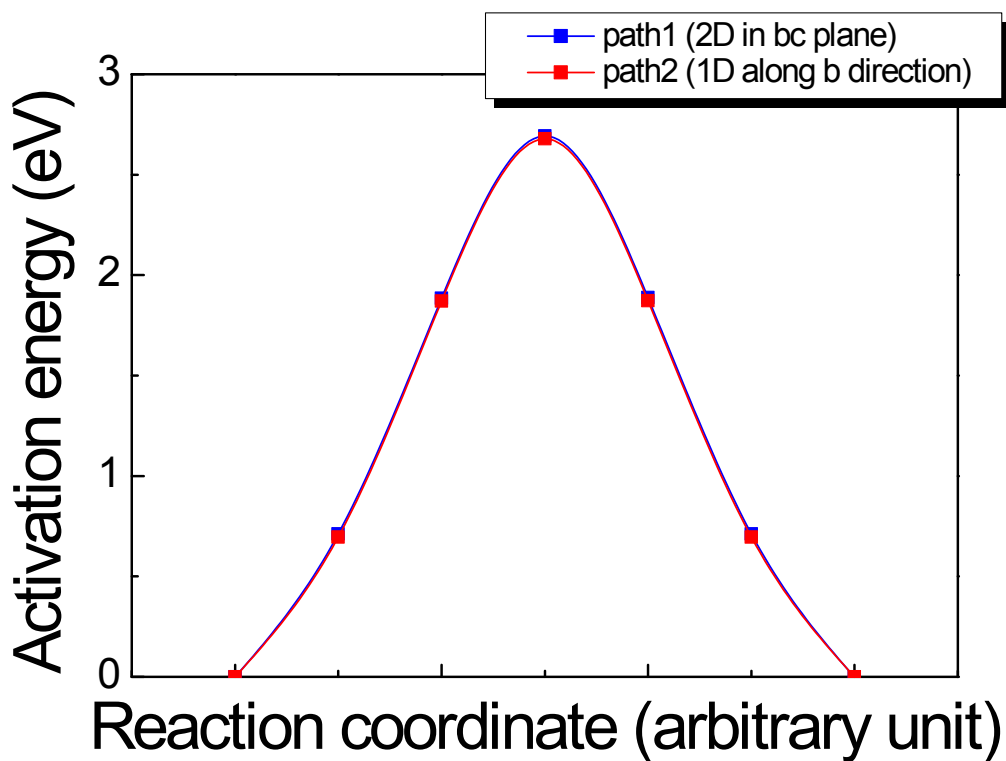


**Figure S7.** The activation barriers for Na hopping along two diffusion pathways of maricite  $\text{Na}_{1-x}\text{FePO}_4$  ( $x \approx 1$ ). The diffusion pathways are presented in Figure 2. The diffusion barriers for Na hopping in maricite  $\text{Na}_{1-x}\text{FePO}_4$  ( $x \approx 1$ ) are much higher than those in maricite  $\text{Na}_{1-x}\text{FePO}_4$  ( $x \approx 0$ ). This seems due to larger electrostatic repulsion between Na and oxidized  $\text{Fe}^{3+}$  ions ( $x \approx 1$ ) than that between Na and  $\text{Fe}^{2+}$  ions ( $x \approx 0$ )

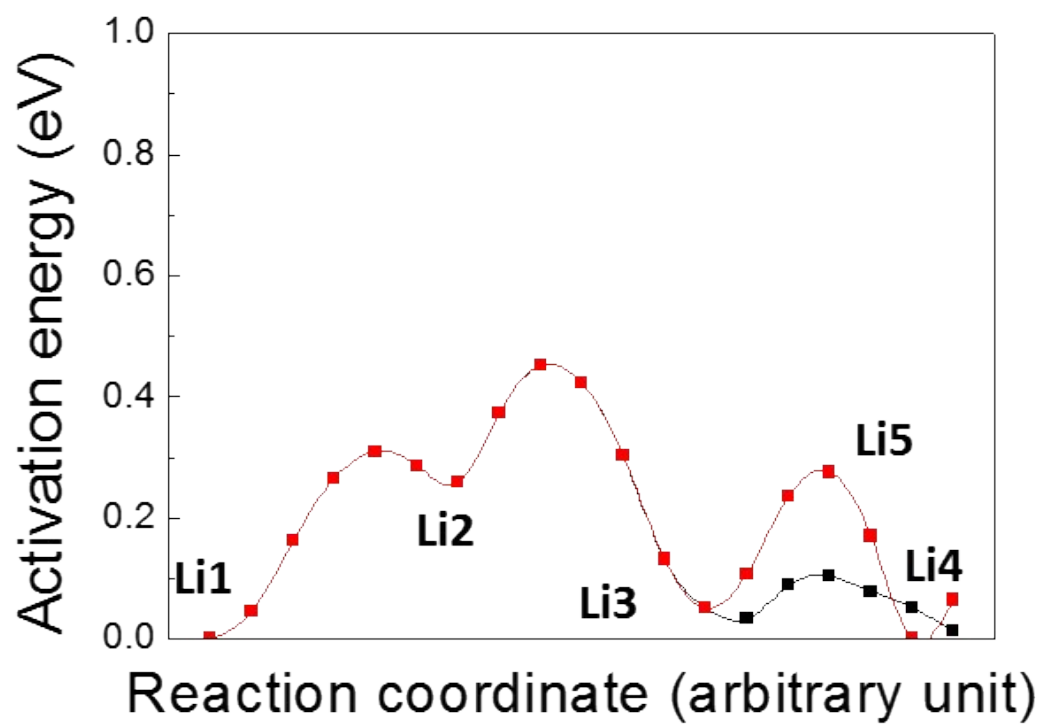


**Figure S8.** The activation barrier for Li ion in  $\alpha$ -FePO<sub>4</sub>. The diffusion pathways for Li ion are same with those for Na ion, as shown in Figure 4.

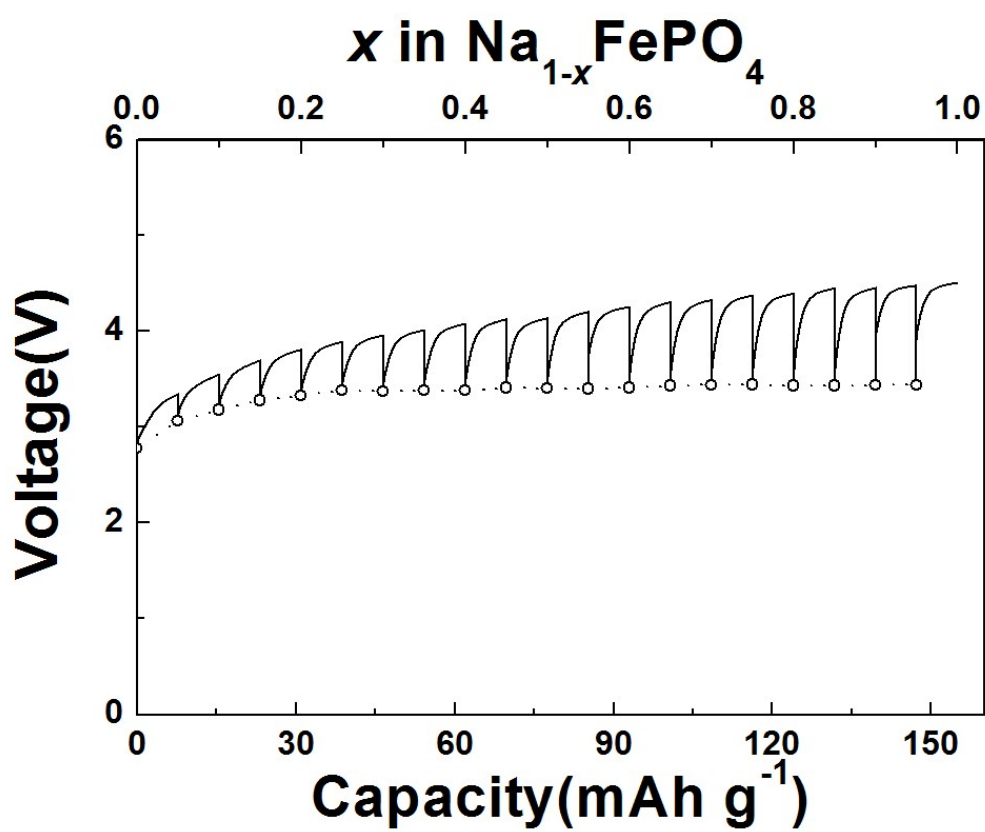


**Figure S9.** GITT of maricite  $\text{NaFePO}_4$  during first charge

Element	Mass fraction(%)
C	20.35

**Table S1.** Carbon analysis of C-NaFePO<sub>4</sub>

---

	Formation energies (eV / f.u.)
Olivine-NaFePO <sub>4</sub>	-47.193
Maricite-NaFePO <sub>4</sub>	-47.196
Olivine-FePO <sub>4</sub>	-42.724
Maricite-FePO <sub>4</sub>	-42.695

---

**Table S2.** Formation energies of various Na<sub>x</sub>FePO<sub>4</sub> ( $x = 0, 1$ )

		<b>Atomic ratio</b>
<b>Fully desodiated maricite NaFePO<sub>4</sub></b>	<b>Na</b>	0.01
	<b>Fe</b>	0.93
	<b>P</b>	1

**Table S3.** Atomic ratio of fully desodiated maricite NaFePO<sub>4</sub>

## References

1. J. P. Perdew, K. Burke and M. Ernzerhof, *Phy. Rev. Lett.*, 1996, **77**, 3865-3868.
2. G. Kresse and J. Furthmuller, *Com. Mater. Sci.*, 1996, **6**, 15-50.
3. S. L. Dudarev, G. A. Botton, S. Y. Savrasov, C. J. Humphreys and A. P. Sutton, *Phy. Rev. B*, 1998, **57**, 1505-1509.
4. F. Zhou, M. Cococcioni, K. Kang and G. Ceder, *Electrochem. Commun.*, 2004, **6**, 1144-1148.
5. S. L. Mayo, B. D. Olafson and W. A. Goddard, *J. Phys. Chem.*, 1990, **94**, 8897-8909.
6. S. Adams, *Solid State Ionics*, 2000, **136**, 1351-1361.
7. I. D. Brown, *Chem. Rev.*, 2009, **109**, 6858-6919.
8. M. Sale and M. Avdeev, *J. Appl. Crystallograph.*, 2012, **45**, 1054-1056.
9. K. Momma and F. Izumi, *J. Appl. Crystallograph.*, 2008, **41**, 653-658.